Calculating Effective Absolute Permeability in Sandstone/Shale Sequences

Clayton Deutsch, Stanford U.

SPE 17264

Summary. Two averaging algorithms are proposed for determining block effective absolute permeability. The experimental relationship between the effective permeability, the volume fraction of shale, and the anisotropy of the shales is first observed through repeated flow simulations. A power-averaging model and a percolation model are proposed to fit the experimentally observed relationship. The power-averaging model provides a surprisingly easy and efficient way to calculate block effective absolute permeability. A simple graph is given to determine the averaging power from the geometric anisotropy (aspect ratio) of the shales for both vertical and horizontal steady-state flow. The effective absolute permeability can then be calculated with the averaging power, the volume fraction of shale, and the component sandstone and shale permeabilities. The effective permeability of a sandstone/shale sequence is affected when the shales are large with respect to the size of the gridblocks. A correction for large shales relative to small gridblocks is also proposed.

Introduction

One goal of reservoir engineering is to develop reservoir-management plans to achieve optimal recovery under certain economic constraints. Reservoir simulation provides the means to perform this optimization by predicting recovery before production. The simulation programs solve mathematical equations that describe the flow of fluids through a numerical model of the reservoir. This paper considers the problem of building an accurate numerical model of absolute permeability.

The problem is difficult because flow-simulation programs implicitly assume that each gridblock is homogeneous. In reality, however, the reservoir unit that each gridblock represents is rarely homogeneous. Therefore, to describe the reservoir accurately, it is necessary to define effective properties that represent the small-scale heterogeneity found within each gridblock. This task is not too difficult if the reservoir is relatively homogeneous. Unfortunately, in the most common clastic reservoir, a sandstone/shale sequence, there are severe discontinuities. The flow transport properties within the constituent shales and sandstone differ drastically.

The sandstone matrix contains the movable fluids, while shales provide obstacles for fluid flow. Neither the sandstone nor the shales are homogeneous. The impact of the heterogeneity within the sandstone and shale, however, is not as important as that of the transition between the sandstone and shale.[1-5] The study presented here will consider the sole heterogeneity introduced by the transition between the two rock types.

The impact of the shales on the block effective absolute permeability will depend on the volume and spatial distribution of the shales. As the volume, V_{sh}, increases, the effective absolute permeability decreases. Other important factors are the shape and orientation of the shales with respect to the direction of fluid flow. The shales have the most impact on vertical flow and the least impact on horizontal flow.

When the shales within a reservoir can be correlated between wells, the reservoir is essentially separated into distinct layers that should be handled separately in the simulation program. The shales that must be accounted for by averaging are the ones that are discontinuous between wells. These discontinuous shales can significantly affect reservoir performance.

Discontinuous shales can be modeled by stochastic processes. To study the effect of discontinuous or stochastic shales on the block effective absolute permeability, various sandstone/shale sequences were simulated and single-phase steady-state flow simulations were performed to obtain effective permeabilities. The relationship between the resultant effective permeability and the volume fraction of shale was then observed for various shale geometries. Two models for the averaging process will be considered: a power-average and a percolation-theory-based model. The resultant models can be applied to real reservoirs to estimate effective absolute permeability.

Calculating Effective Absolute Permeability

The sandstone/shale sequence is modeled as a three-dimensional (3D) grid network where each gridblock is either sandstone or shale. A particular sandstone/shale sequence is created by adding shales of a given geometry and orientation until a specified target volume fraction is met. Shales are assumed to be ellipsoids of equal size and are positioned independently of other shales. The shale geometry may look quite complex because of overlapping of the shale units and truncation of the shales on the boundary of the grid network. These effects are illustrated in Fig. 1, which shows two horizontal and two vertical sections from a particular sandstone/shale configuration.

After the sandstone/shale configuration is created, the effective permeability is found by observing the steady-state flow rate for an applied pressure gradient. The commercial flow simulator ECLIPSE has been used to determine the steady-state flow rate. The block effective permeability can then be calculated directly from Darcy's law. The outlined procedure can be repeated with different volume fractions of shale. Thus, the relationship between the effective permeability and the volume fraction of shale is empirically observed rather than analytically derived.

The relationship between the effective permeability and the proportion of shale for small isotropic shales (i.e., each shale is the size of an elemental cubic grid unit) is shown in Fig. 2. The permeability of each gridblock in the $20\times20\times10$ network is assigned either a sandstone permeability (1,000 md) or a shale permeability (0.01 md) before flow simulation. The three traditional averaging processes (the arithmetic, geometric, and harmonic averages) are shown for reference. Although none of the three conventionally used averages adequately represents the effective permeability, a clear functional relation appears between the effective permeability and the volume fraction of shale for $V_{sh}<0.4$.

Commonly occurring shales are highly anisotropic and are not spatially uncorrelated as in the previous simulation. Figs. 3 and 4 show the results of models constructed for directions parallel and perpendicular to the major anisotropy. A 10:1 horizontal-to-vertical anisotropy ratio was considered for the shale geometry, with an equal range in all horizontal directions. The horizontal permeability (parallel to the major direction of continuity) is consistently greater than the vertical permeability. The arithmetic average appears to represent the horizontal permeability adequately for shale volumes <40%. The vertical permeability also appears clearly related to the volume fraction of shale for $V_{sh}<40\%$ but cannot be modeled with conventional averaging techniques. The numerical results presented in Figs. 2 through 4 suggest that an averaging process can be defined that varies continuously with the degree of shale continuity.

Modeling the Averaging Process

Two different techniques (power averaging and a percolation model) are presented to model the observed behavior between the effective permeability and the volume fraction of shale.

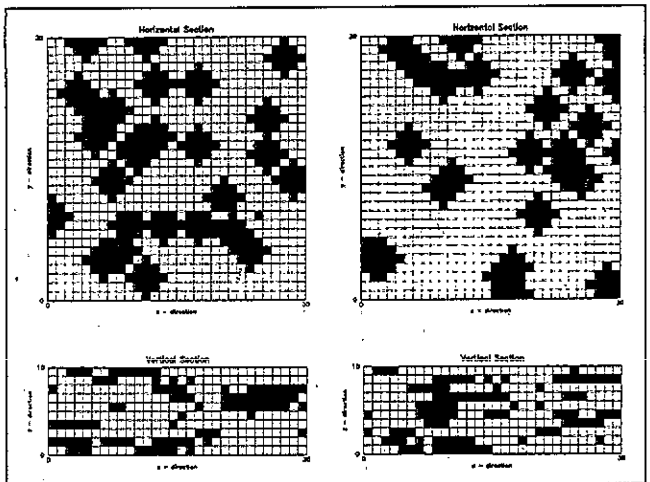

Fig. 1—Two horizontal and two vertical cross sections of a simulated sandstone/shale sequence are shown. Note the complex geometry created by overlapping and truncation of the shales. The dimensions of an elemental shale unit are 5×5 in the x-y directions and 1 in the z (vertical) direction.

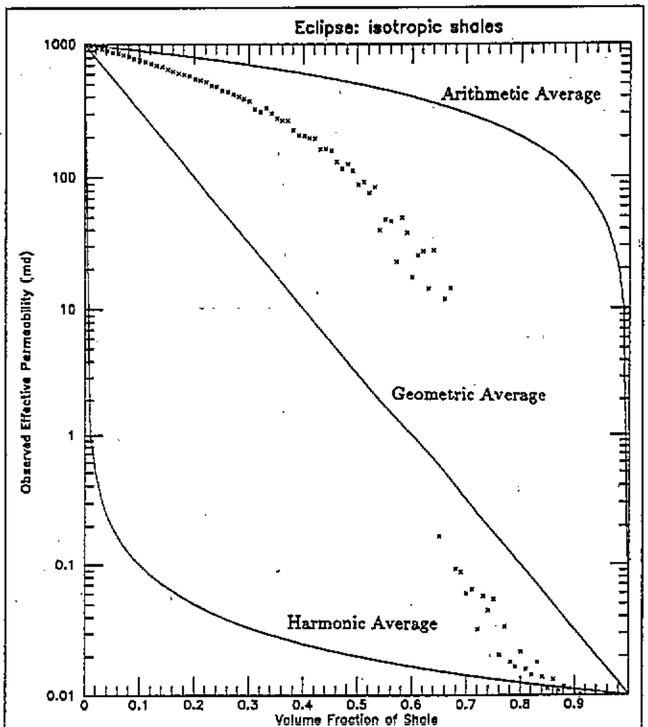

Fig. 2—k_e vs. V_{sh}. Shales are added randomly to a reservoir grid (20×20×10). k_e is then calculated by flow simulation. The three common averages are shown for reference. Note the clear relation between k_e and V_{sh} for $V_{sh}<40\%$ and the percolation behavior near the critical threshold $V_{shc}=0.69$.

Power Averaging. One straightforward approach is to model the effective permeability, k_e, as a power average of the component permeabilities:

$$k_e=[V_{sh}k_{sh}^{\omega}+(1-V_{sh})k_{ss}^{\omega}]^{1/\omega}, \quad \text{(1)}$$

where k_{sh} and k_{ss} = shale and sandstone permeabilities, respectively, V_{sh} = volume fraction of shale, and ω = some averaging power. Korvin[6] presents the axiomatic foundations of the method and discusses various applications in the earth sciences. Journel *et al.*[7] and Deutsch[8] show power averaging to be a viable approach to estimate effective absolute permeability.

The effective permeability, k_e, of a 3D network of blocks, each with a known permeability, may take any value between the har-

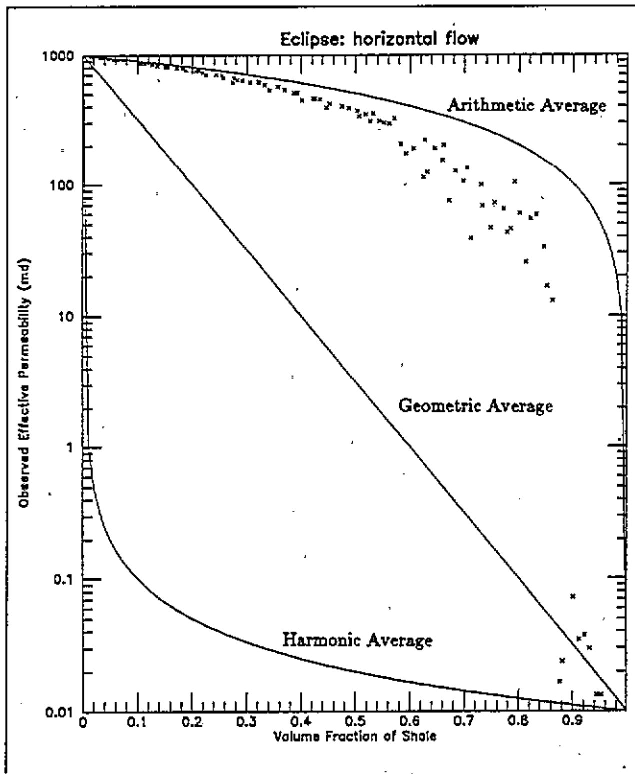

Fig. 3—$k_{e,H}$ vs. V_{sh}. Anisotropic shales have been added to a sandstone matrix to simulate a sandstone/shale sequence (the network size is 20×20×10). The shales have a circular horizontal cross section 10 units in diameter and a 1-unit vertical thickness. Thus, the shales have a 10:1 horizontal-to-vertical anisotropy. The three common averages are shown for reference. Note the clear relation between k_e and V_{sh} for $V_{sh}<40\%$.

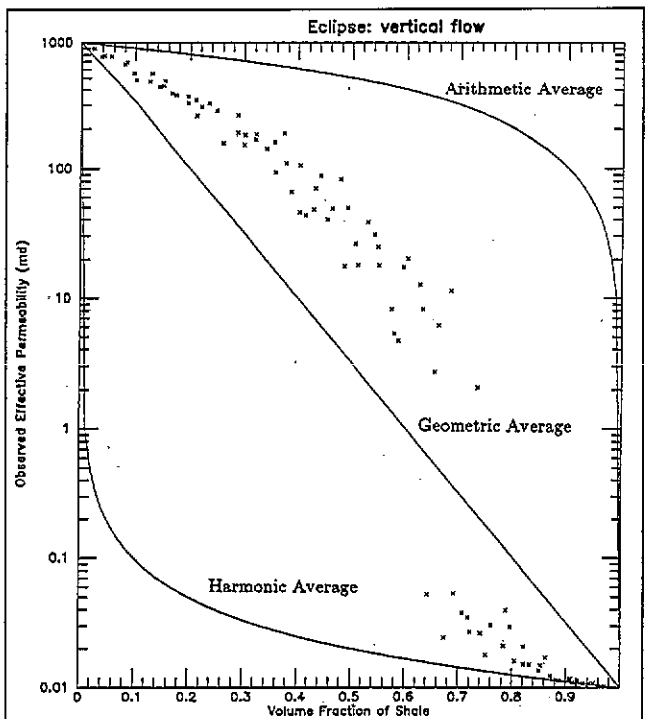

Fig. 4—$k_{e,V}$ vs. V_{sh}. The simulation setting is the same as for Fig. 3. Note the clear relation between k_e and V_{sh} for $V_{sh}<40\%$ and the difference between these results and the results for horizontal flow shown in Fig. 3.

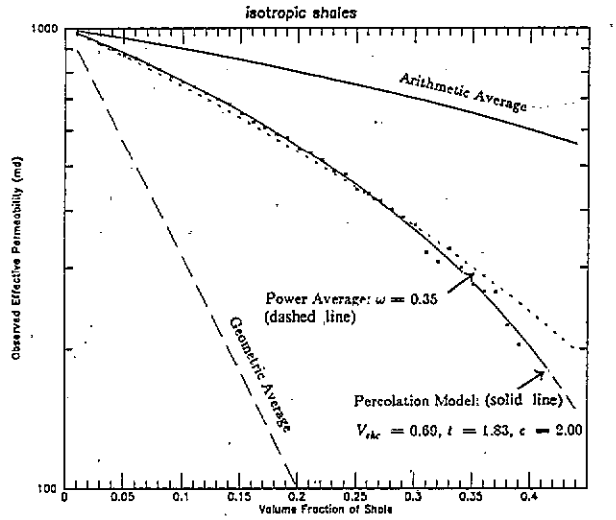

Power Average: $k_e = \left(V_{sh} \cdot k_{sh}^{\omega} + (1 - V_{sh}) \cdot k_{ss}^{\omega} \right)^{\frac{1}{\omega}}$

Percolation Model: $k_e = k_{ss} \cdot c \cdot (V_{shc} - V_{sh})^t$

Fig. 5—k_e vs. V_{sh}. This graph shows the same results as Fig. 2 with more detail for $V_{sh}<40\%$. A power-average model and the percolation-theory model are shown to provide an extremely good fit to the experimental results.

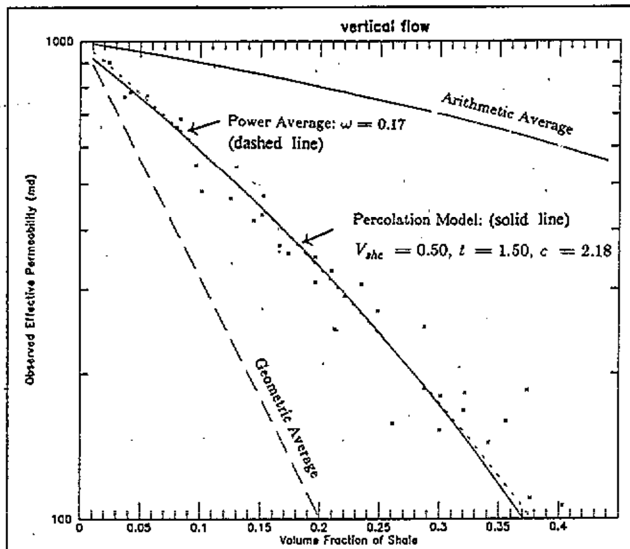

Power Average: $k_e = \left(V_{sh} \cdot k_{sh}^{\omega} + (1 - V_{sh}) \cdot k_{ss}^{\omega} \right)^{\frac{1}{\omega}}$

Percolation Model: $k_e = k_{ss} \cdot c \cdot (V_{shc} - V_{sh})^t$

Fig. 7—$k_{e,V}$ vs. V_{sh}. This graph shows the same results as Fig. 4 with more detail for $V_{sh}<40\%$. The power-average model and the percolation-theory model provide a good fit to the experimental results.

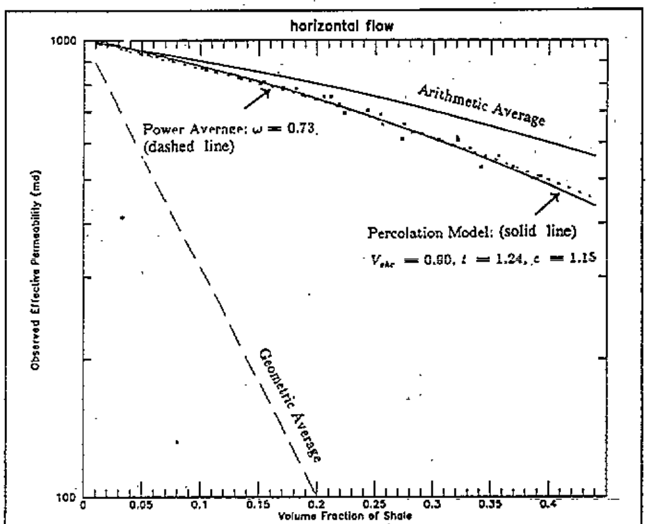

Power Average: $k_e = \left(V_{sh} \cdot k_{sh}^{\omega} + (1 - V_{sh}) \cdot k_{ss}^{\omega} \right)^{\frac{1}{\omega}}$

Percolation Model: $k_e = k_{ss} \cdot c \cdot (V_{shc} - V_{sh})^t$

Fig. 6—$k_{e,H}$ vs. V_{sh}. This graph shows the same results as Fig. 3 with more detail for $V_{sh}<40\%$. The power-average model and the percolation-theory model are again shown to fit the experimental results well.

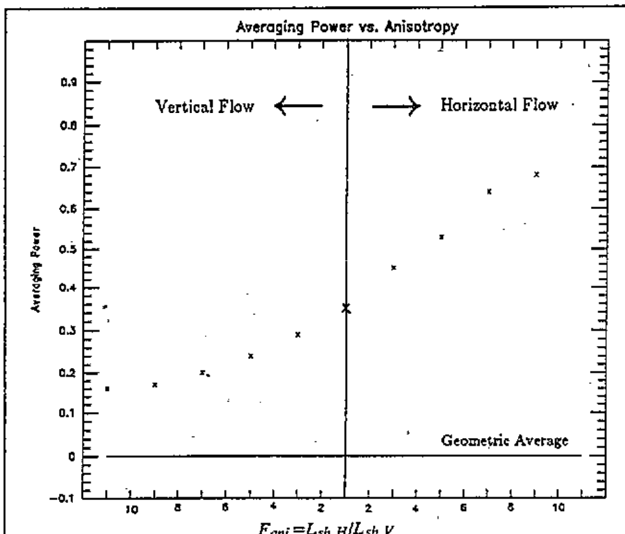

Fig. 8—The relationship between the averaging power ω and the anisotropy F_{ani}. The blocks used in the simulation are $20\times20\times10$. The right side is for horizontal flow and the left side is for vertical flow. If the anisotropy of the shales can be inferred, then the correct averaging powers can be read. Eq. 1 can then be used to provide an estimate for the block k_e.

monic and arithmetic average of the block permeabilities, depending on their spatial arrangement. The lower-bound harmonic average can be seen as a power average with $\omega=-1$. Similarly, the upper-bound arithmetic average can be seen as a power average with the power $\omega=+1$. The geometric average is obtained with a power $\omega=0$ average (through a limited expansion, because Eq. 1 is not defined for $\omega=0$). Therefore, the effective permeability is given by a power ω average with a power value ω between -1 and $+1$. The problem of determining the effective permeability is now solved if the volume of shale, the component sandstone and shale permeabilities, and the averaging power are known.

Percolation Model. Percolation theory considers the general problem of fluid flowing through some heterogeneous medium.[9] Subsurface flow of water or oil through a sandstone/shale sequence is one example, and the flow of electricity through a resistor network is another example. On the basis of numerical results, Kirkpatrick[10] proposes a power law to describe the normalized electrical conductance of a resistor network. In the context of effective absolute permeability, Kirkpatrick's relationship can be written as

$$k_e/k_{ss}=c(V_{shc}-V_{sh})^t, \quad \ldots\ldots (2)$$

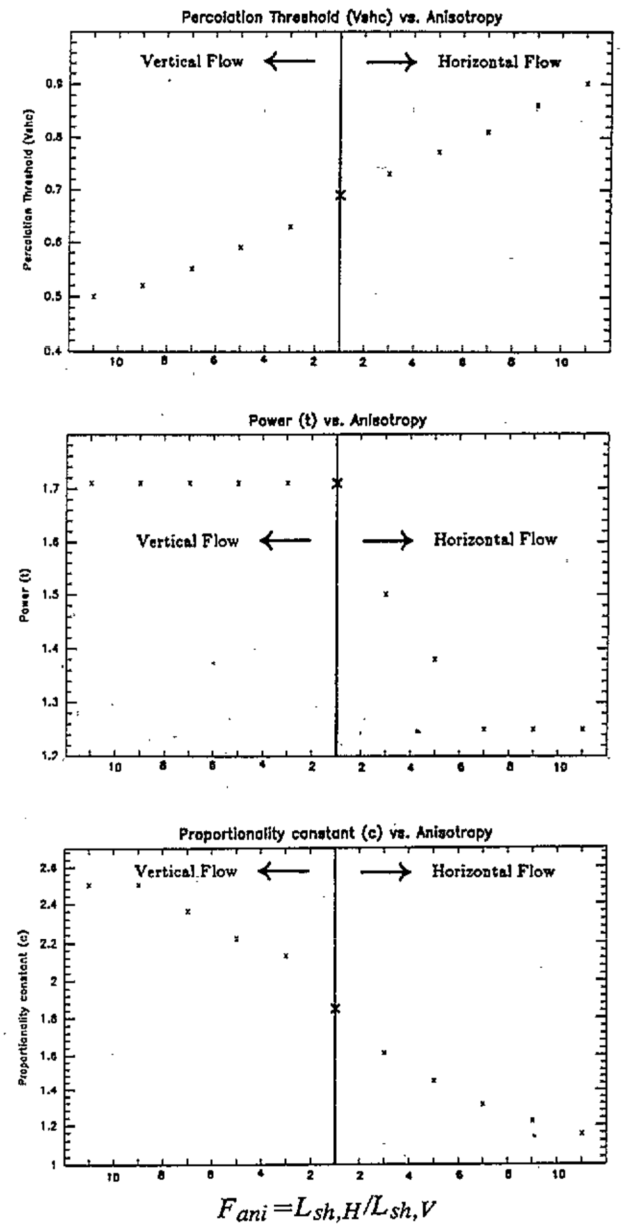

Fig. 9—The relationship between V_{shc}, t, and c and F_{ani}. The simulation conditions are the same as for Fig. 8. The right side corresponds to horizontal flow and the left side to vertical flow. Knowing F_{ani}, the appropriate parameters for Model 2 can be read.

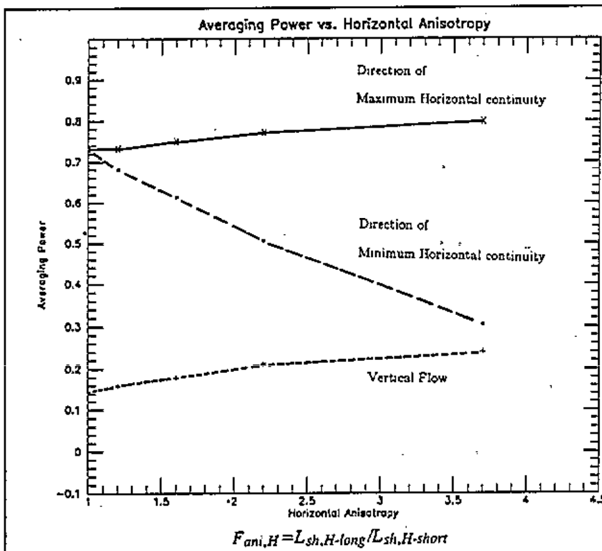

Fig. 10—The relationship between ω and $F_{ani,H}$. The vertical-to-horizontal anisotropy ratio as defined in Eq. 3 is held constant at 10. Note the effect of horizontal anisotropy on the averaging for all three block directions.

where V_{shc}=critical volume fraction of shale, t=an exponent (near 1.5 to 2.0), and c=a proportionality constant (near 1.5 to 2.0). The critical shale fraction is the maximum amount of shale beyond which the flow rate will drop dramatically: V_{shc}=0.69 in Fig. 2. From Figs. 3 and 4, we see that the critical threshold changes with anisotropic shales. As the spatial continuity in the direction of flow increases, so does the critical threshold.

The critical threshold can be predicted by percolation theory for some very simple configurations. For example, the critical threshold for random, isotropic shales in a two-dimensional (2D) space[11] is V_{shc}=0.5. For spatially correlated heterogeneities in a 3D space, percolation-theory results are not yet established. The percolation model (Eq. 2) will be extended to cases where no theoretical threshold value exists, and the corresponding parameters (V_{shc}, c, and t) will be fitted to the experimental results.

Some Numerical Results. Fig. 5 shows the results of using the power-average and percolation models. Regression analysis indicates a good fit between the modeling averages and the empirical sandstone/shale permeability data. Figs. 6 and 7 show the best-fitting models for the anisotropic results presented in Figs. 3 and 4. In both cases, the power-average and the percolation models provide very good approximations to the numerical results.

Additional cases with different anisotropy ratios were considered to establish the relation between the model parameters (ω, V_{shc}, c, and t) and the anisotropy ratio. The anisotropy ratio, F_{ani}, is defined as the longest shale dimension (horizontal) divided by the shortest shale dimension (vertical):

$$F_{ani} = L_{sh,H}/L_{sh,V}. \qquad (3)$$

Fig. 8 shows how the averaging power, ω, depends on the anisotropy ratio, F_{ani}. The averaging power for horizontal flow and vertical flow are shown on opposite sides of the graph. As the anisotropy ratio increases beyond some maximum, the averaging power is seen to change very little. If F_{ani} went to ∞, the arithmetic ($\omega=1$) and harmonic ($\omega=-1$) averages would be found for horizontal and vertical permeability, respectively. These limit cases, however, would correspond to a perfectly layered sandstone/shale sequence, which is not of interest to this study. The averaging power for vertical flow is seen to be very far from the theoretical minimum of -1. The harmonic average would be obtained when the shales are aligned perfectly opposite the flow. This never happens with discontinuous shales because there are always tortuous paths that the fluid can follow through the sandstone. It appears that the geometric average (ω=0) traditionally used for vertical flow underestimates the effective vertical permeability. To consider large anisotropy ratios ($F_{ani}>11$), it would be necessary to use grid sizes larger than 20×20×10. This was not possible with the computer available to this project.

The percolation threshold, V_{shc}, is a clearly defined physical constant; therefore, it is established before the other two parameters are fitted by least-squares regression. Fig. 9 shows the relationship between the percolation-model parameters (V_{shc}, c, and t) and the anisotropy ratio, F_{ani}. In Fig. 9, it appears that for $F_{ani}<6$, both the critical threshold V_{shc} and the proportionality factor c vary linearly. The power t is found to be constant around 1.71 for vertical flow and to decrease sharply from 1.71 to 1.25, where it stabilizes, for horizontal flow. The physical interpretation of the two parameters c and t, and thus their behavior in Fig. 9, is not yet understood.

In the preceding flow simulations, the shales were all considered to be isotropic in the horizontal plane. To illustrate the effect of anisotropic horizontal shale length on the directional permeability, the anisotropy ratio, F_{ani}, as defined in Eq. 3, will be kept constant at F_{ani}=10 and the second horizontal length will be progressively reduced.

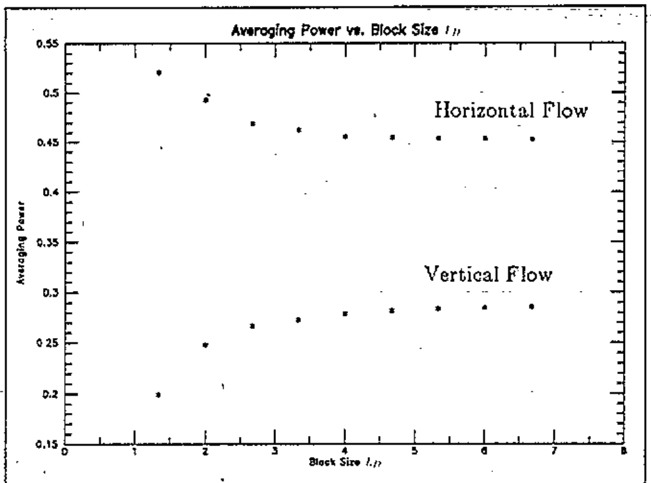

Fig. 11—ω vs. L_D (the results for both horizontal and vertical flow are shown). For blocks with horizontal dimensions larger than three times the shale length ($L_D=3$), the averaging power stabilizes.

When the shales are anisotropic in the horizontal plane, the effective permeability will be different for each of the three grid directions. Fig. 10 shows the averaging power ω for each grid direction vs. the horizontal anisotropy (recall that F_{ani} is fixed at 10). Note that (1) the permeability in the direction of maximum shale continuity is the largest and the permeability in the direction of minimum shale continuity is the smallest and (2) the vertical permeability increases (for a given F_{ani}) with increasing horizontal anisotropy.

In practice there may be information on the directional horizontal dimension of the shales. The directional permeability can then be corrected in the manner described. One further correction may be required because of the size of the shales relative to the size of the simulation gridblocks.

Effect of Block Size. All numerical flow simulations must consider a finite grid size. In some cases, the shales will not be small with respect to the size of the gridblock. We know that the effective properties of a bounded medium depend on the ratio of the autocovariance range (e.g., size of the shales) to the block dimension. Smith and Freeze[12] discuss this for one-dimensional and 2D flow. Desbarats[3] illustrates the effect for 3D flow.

The dimension of the shales and the autocovariance range are equivalent when the shale centers are located independently. This is the case for the simulations generated in this paper. Therefore, a dimensionless block length can be defined as the ratio of the block length to the length of the elemental shales:

$$L_D=L_b/L_{sh}. \quad (4)$$

From the numerical results noted,[3,12] it is known that if $L_D>2$ or 3, there will be no noticeable change in the effective properties. This would suggest that the block size should be selected greater than three times the shale size to filter out the influence of the grid size. This corresponds to the notion of a representative elemental volume.

Fig. 11 shows how the averaging power ω varies with the block size L_D for shales with a fixed 3:1 anisotropy ratio (i.e., $F_{ani}=3$).

1. For horizontal flow, the power ω decreases to an asymptotic minimum as L_D becomes large. The minimum is reached around $L_D=3$.

2. In practice, the dimensionless block length for the vertical direction is always large (i.e., $L_D>10$). In Fig. 11, we are seeing the effect of the horizontal dimensionless block length on the vertical flow behavior. The averaging power ω increases to a maximum as L_D becomes large ($L_D>3$).

From this example, some general conclusions can be made regarding the effect of the block size. First, we see that if the block length is less than three times the shale length, the effective permeability is affected. For horizontal flow, the effective permeability is greater than that obtained for the "large-block" domain

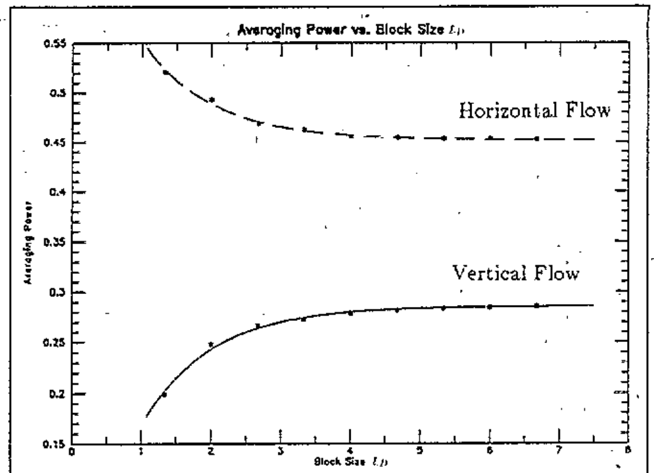

$$\omega_{acor} = (1 + a \cdot e^{-L_D}) \cdot \omega$$

Horizontal Flow: $\omega = 0.45$ and $a = 0.60$

Vertical Flow: $\omega = 0.29$ and $a = -1.11$

Fig. 12—ω vs. L_D. The results of Fig. 11 are modeled with an exponential correction function.

($L_D>3$); conversely, the vertical permeability is smaller than that for the large-block domain. If the shales are larger than the gridblock (i.e., $L_D<1$), they can be handled explicitly in the flow simulation.

The effect has been shown for only one anisotropy ratio ($F_{ani}=3$). It is clear, however, that this effect will occur for all anisotropy ratios. To account for this effect, a correction to the averaging power is proposed:

$$\omega_{acor}=F_b\omega, \quad (5)$$

where ω_{acor}=corrected averaging power, ω=limit averaging power corresponding to large block, and F_b=block correction factor. The block correction factor, F_b, can be obtained either directly from charts or figures (e.g., Fig. 11) or from a mathematical relation of the form

$$F_b=1+ae^{L_D}, \quad (6)$$

where a=constant that measures the amount of correction needed. As the relative block size L_D becomes large ($L_D>3$), the block correction factor F_b will be equal to 1. The constant a will be positive for horizontal flow and negative for vertical flow—e.g., constant a would be $+0.60$ and -1.11 for the horizontal and vertical flow results, respectively, shown in Fig. 11. Fig. 12 shows the resultant models.

The effect of the block dimension relative to the shale dimension has been addressed. If the size of the block is small or if the shales are large, the limit averaging power corresponding to large blocks must be corrected. A negative exponential correction is proposed to provide this correction.

Discussion of Results. A large block size and isotropic horizontal shales are assumed to be reasonable first approximations. When detailed information about the relative block size or horizontal anisotropy is available, however, it can be used to refine the estimate of the averaging process. Both the power-average model and the percolation-type model provide a good fit to the experimental results. However, one additional question remains: which of these two models should be used?

There are several reasons to use the power-average approach.

1. The power-average is the most parsimonious (one parameter vs. three). A procedure that requires evaluation of a single parameter, ω, is extremely easy to implement.

2. The shale permeability does not have to be set to zero, as required by the percolation model.

3. The power-averaging algorithm can be extended to a multimodal or continuous distribution of permeability.

The percolation model is not easily generalized to the case of a multimodal permeability distribution. There are, however, several reasons to use the percolation model.

1. The model is continuous until the percolation threshold V_{shc}. This allows estimation of permeability for very shaly sequences.

2. Because the percolation model relies on three parameters rather than one, the model gives the lowest mean-squared error when experimental data are fitted.

The drawback of the percolation model is that three parameters must be estimated. Estimating the parameters is complicated because the estimate of one parameter will affect the choice of the others.

The power-averaging model is the simplest and most practical. Averaging powers, ω, can be estimated from such charts as Fig. 8. The effective permeability can then be obtained from Eq. 1. The improvements over the traditional arithmetic and geometric averages can be appreciated from Figs. 6 and 7.

Conclusions

For sandstone/shale sequences, a major problem is that of averaging the component sandstone and shale permeabilities to obtain block effective permeabilities. Typically, a geometric average ($\omega=0$) is used for vertical permeability and an arithmetic average ($\omega=1$) is used for the horizontal permeability. Results from flow simulation make it clear that this approach can be improved if the anisotropy of the shales is accounted for. Two models have been proposed to account for the shale anisotropy.

The averaging process for absolute permeability in sandstone/shale sequences can be modeled by either a power-average or a percolation model. The power-averaging model is recommended because of its simplicity and effectiveness. The important aspect of this averaging problem is the presence of two rock components. The preliminary results of this research require certain limiting assumptions: the sandstone and shales are assumed to be homogeneous, and the shales are assumed to be located independently from each other with the same elliptical shape and orientation. By making the averaging process depend on the spatial anisotropy, more information can be used and a better estimate of effective permeability in sandstone/shale sequences can be obtained. Thus, the reservoir model will be more accurate and predictions from flow-simulation programs are more likely to reflect future reservoir performance.

Nomenclature

a = constant used for block-size correction
c = proportionality constant
F_{ani} = anisotropy ratio
F_b = block-size correction factor
k_e = block effective permeability, md
k_{sh} = shale permeability, md
k_{ss} = sandstone permeability, md
L_b = block length
L_D = dimensionless block length
L_{sh} = shale length
t = percolation-model parameter
V_{sh} = volume fraction of shale
V_{shc} = critical volume fraction of shale
ω = averaging power between -1 and $+1$
ω_{acor} = averaging power corrected for block size

Subscripts

H = horizontal
r = relative
V = vertical

Acknowledgments

Acknowledgment is made to the donors of the Petroleum Research Fund, administered by the American Chemical Society, for support of this research. Additional support was provided by the Stanford Center for Research Forecasting. I thank A.G. Journel for his helpful comments and suggestions on this work.

References

1. Fogg, G.E.: "Groundwater Flow and Sand Body Interconnectedness in a Thick Multiple Aquifer System," *Water Resources Res.* (Oct. 1986) **22,** No. 5, 679–94.
2. Haldorsen, H.H. and Lake, L.W.: "A New Approach to Shale Management in Field-Scale Models," *SPEJ* (Aug. 1984) 447–57.
3. Desbarats, A.J.: "Numerical Estimation of Effective Permeability in Sand-Shale Formations," *Water Resources Res.* (Feb. 1987) **23,** No. 2, 273–86.
4. Warren, J.E. and Price, H.S.: "Flow in Heterogeneous Porous Media," *SPEJ* (Sept. 1961) 153–69; *Trans.*, AIME, **222.**
5. Weber, K.J.: "Influence of Common Sedimentary Structures on Fluid Flow in Reservoir Models," *JPT* (March 1982) 665–72.
6. Korvin, G.: "Axiomatic Characterization of the General Mixture Rule," *Geoexploration* (1981) **19,** 267–76.
7. Journel, A.G., Deutsch, C.V., and Desbarats, A.J.: "Power Averaging for Block Effective Permeability," paper SPE 15128 presented at the 1986 SPE California Regional Meeting, Oakland, April 2–4.
8. Deutsch, C.V.: "Estimating Block Effective Permeability With Geostatistics and Power Averaging," paper SPE 15991 available at SPE, Richardson, TX.
9. Hammersley, J.M. and Welsh, D.J.A.: "Percolation Theory and its Ramifications," *Contemp. Phys.* (1980) **21,** No. 6, 593–605.
10. Kirkpatrick, S.: "Percolation and Conduction," *Reviews of Modern Physics* (1973) **45,** No. 4, 574–88.
11. Sykes, M.F. and Essam, J.W.: "Exact Critical Percolation Probabilities for Site and Bond Problems in Two Dimensions," *J. Math Phys.* (1964) **5,** 1117–27.
12. Smith, L. and Freeze, R.A.: "Stochastic Analysis of Steady State Groundwater Flow in a Bounded Domain 1: One Dimensional Simulations," *Water Resources Res.* (Dec. 1979) **15,** No. 6, 1543–59.

SPEFE

Original SPE manuscript received for review Sept. 14, 1987. Paper (SPE 17264) accepted for publication May 18, 1988. Revised manuscript received Aug. 19, 1988.

3. The power-averaging algorithm can be extended to a multimodal or continuous distribution of permeability.

The percolation model is not easily generalized to the case of a multimodal permeability distribution. There are, however, several reasons to use the percolation model.

1. The model is continuous until the percolation threshold V_{shc}. This allows estimation of permeability for very shaly sequences.

2. Because the percolation model relies on three parameters rather than one, the model gives the lowest mean-squared error when experimental data are fitted.

The drawback of the percolation model is that three parameters must be estimated. Estimating the parameters is complicated because the estimate of one parameter will affect the choice of the others.

The power-averaging model is the simplest and most practical. Averaging powers, ω, can be estimated from such charts as Fig. 8. The effective permeability can then be obtained from Eq. 1. The improvements over the traditional arithmetic and geometric averages can be appreciated from Figs. 6 and 7.

Conclusions

For sandstone/shale sequences, a major problem is that of averaging the component sandstone and shale permeabilities to obtain block effective permeabilities. Typically, a geometric average ($\omega=0$) is used for vertical permeability and an arithmetic average ($\omega=1$) is used for the horizontal permeability. Results from flow simulation make it clear that this approach can be improved if the anisotropy of the shales is accounted for. Two models have been proposed to account for the shale anisotropy.

The averaging process for absolute permeability in sandstone/shale sequences can be modeled by either a power-average or a percolation model. The power-averaging model is recommended because of its simplicity and effectiveness. The important aspect of this averaging problem is the presence of two rock components. The preliminary results of this research require certain limiting assumptions: the sandstone and shales are assumed to be homogeneous, and the shales are assumed to be located independently from each other with the same elliptical shape and orientation. By making the averaging process depend on the spatial anisotropy, more information can be used and a better estimate of effective permeability in sandstone/shale sequences can be obtained. Thus, the reservoir model will be more accurate and predictions from flow-simulation programs are more likely to reflect future reservoir performance.

Nomenclature

a = constant used for block-size correction
c = proportionality constant
F_{ani} = anisotropy ratio
F_b = block-size correction factor
k_e = block effective permeability, md
k_{sh} = shale permeability, md
k_{ss} = sandstone permeability, md
L_b = block length
L_D = dimensionless block length
L_{sh} = shale length
t = percolation-model parameter
V_{sh} = volume fraction of shale
V_{shc} = critical volume fraction of shale
ω = averaging power between -1 and $+1$
ω_{acor} = averaging power corrected for block size

Subscripts

H = horizontal
r = relative
V = vertical

Acknowledgments

Acknowledgment is made to the donors of the Petroleum Research Fund, administered by the American Chemical Society, for support of this research. Additional support was provided by the Stanford Center for Research Forecasting. I thank A.G. Journel for his helpful comments and suggestions on this work.

References

1. Fogg, G.E.: "Groundwater Flow and Sand Body Interconnectedness in a Thick Multiple Aquifer System," *Water Resources Res.* (Oct. 1986) **22**, No. 5, 679–94.
2. Haldorsen, H.H. and Lake, L.W.: "A New Approach to Shale Management in Field-Scale Models," *SPEJ* (Aug. 1984) 447–57.
3. Desbarats, A.J.: "Numerical Estimation of Effective Permeability in Sand-Shale Formations," *Water Resources Res.* (Feb. 1987) **23**, No. 2, 273–86.
4. Warren, J.E. and Price, H.S.: "Flow in Heterogeneous Porous Media," *SPEJ* (Sept. 1961) 153–69; *Trans.*, AIME, **222**.
5. Weber, K.J.: "Influence of Common Sedimentary Structures on Fluid Flow in Reservoir Models," *JPT* (March 1982) 665–72.
6. Korvin, G.: "Axiomatic Characterization of the General Mixture Rule," *Geoexploration* (1981) **19**, 267–76.
7. Journel, A.G., Deutsch, C.V., and Desbarats, A.J.: "Power Averaging for Block Effective Permeability," paper SPE 15128 presented at the 1986 SPE California Regional Meeting, Oakland, April 2–4.
8. Deutsch, C.V.: "Estimating Block Effective Permeability With Geostatistics and Power Averaging," paper SPE 15991 available at SPE, Richardson, TX.
9. Hammersley, J.M. and Welsh, D.J.A.: "Percolation Theory and its Ramifications," *Contemp. Phys.* (1980) **21**, No. 6, 593–605.
10. Kirkpatrick, S.: "Percolation and Conduction," *Reviews of Modern Physics* (1973) **45**, No. 4, 574–88.
11. Sykes, M.F. and Essam, J.W.: "Exact Critical Percolation Probabilities for Site and Bond Problems in Two Dimensions," *J. Math Phys.* (1964) **5**, 1117–27.
12. Smith, L. and Freeze, R.A.: "Stochastic Analysis of Steady State Groundwater Flow in a Bounded Domain 1: One Dimensional Simulations," *Water Resources Res.* (Dec. 1979) **15**, No. 6, 1543–59.

SPEFE

Original SPE manuscript received for review Sept. 14, 1987. Paper (SPE 17264) accepted for publication May 18, 1988. Revised manuscript received Aug. 19, 1988.

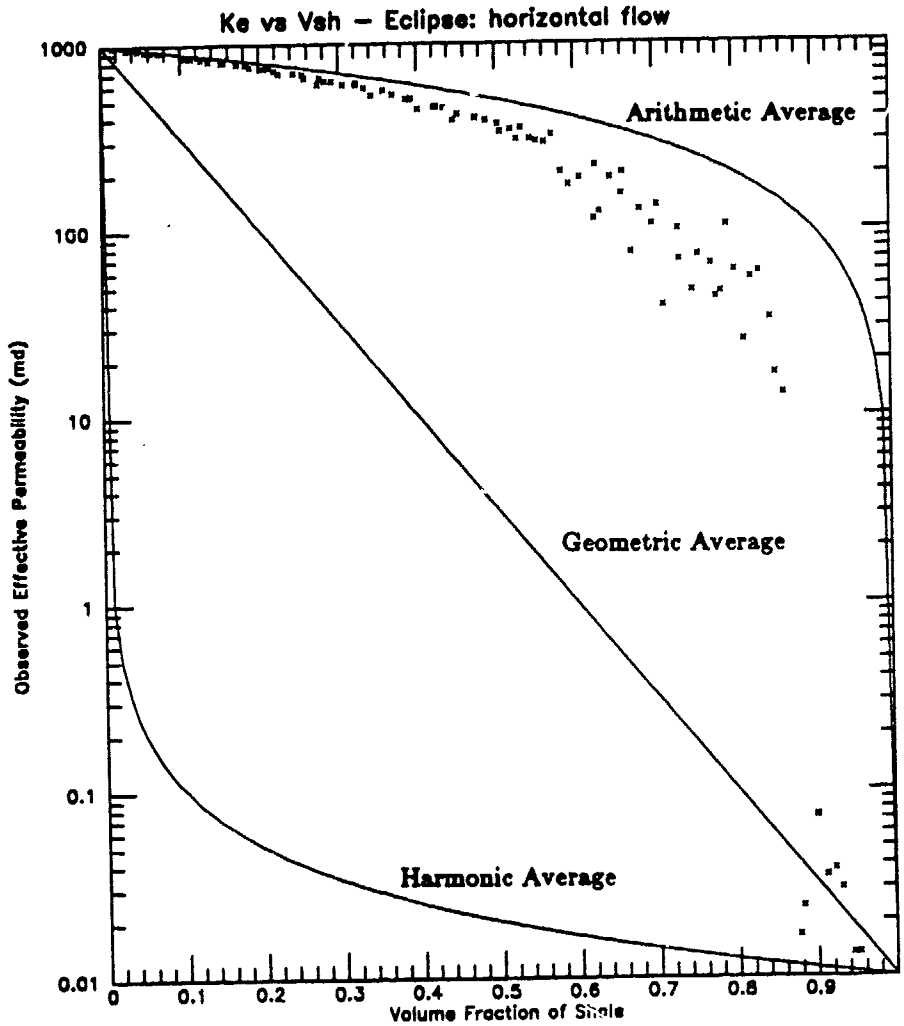

Figure 3: Horizontal effective absolute permeability K_e versus shale volume fraction V_{sh}. Anisotropic shales have been added to a sandstone matrix to simulate a sandstone/shale sequence (the network size is 20x20x10). The shales have a circular horizontal cross-section 10 units in diameter and a 1 unit vertical thickness. Thus, the shales have a 10:1 horizontal to vertical anisotropy. The three common averages (Arithmetic, Harmonic, Geometric) are shown for reference. Note the clear relation between K_e and V_{sh} for $V_{sh} < 40\%$.

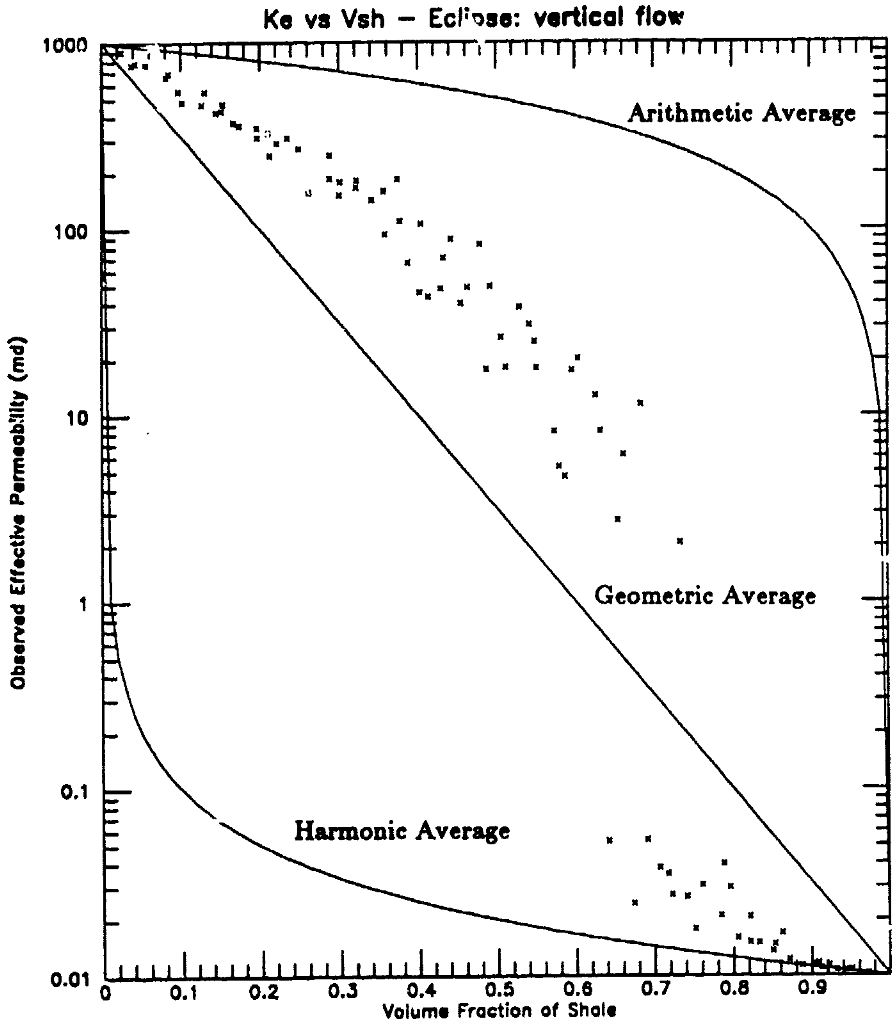

Figure 4: Vertical efective absolute permeability K_e versus shale volume fraction V_{sh}. The simulation setting is the same as for Figure 3. Note the clear relation between K_e and V_{sh} for $V_{sh} < 40\%$ and the difference between these results and the results for horizontal flow shown on Figure 3.

be a viable approach to this problem by Journel, et.al., 1985, and Deutsch, 1986.

The effective permeability K_e of a three dimensional network of blocks, each with a known permeability, may take any value between the harmonic and arithmetic average of the block permeabilities depending on their spatial arrangement. The lower bound harmonic average can be seen as a power average with $\omega = -1$. Similarly, the upper bound arithmetic average can be seen as a power average with the power $\omega = +1$. The geometric average is obtained with a power $\omega = 0$ average (through a limited expansion since equation 1 is not defined for $\omega = 0$). Therefore, the effective permeability is given by a power ω average with a power value ω between -1 and +1. The problem of determining the effective permeability is now mapped into the problem of determining the proportion of shale and the averaging power.

Percolation Model:

Percolation theory was introduced by Broadbent and Hammersley (1957). Percolation theory considers the very general problem of fluid flowing through some heterogeneous medium. The first example studied by Broadbent and Hammersley (1957) was the flow of gas through porous carbon granules. Other examples of fluid flow include the flow of electrons in heterogeneous semiconductors or the flow of messages in an unreliable network. In this paper, the fluid is considered to be water or oil and the medium a sandstone/shale sequence.

There are two ways to describe the randomness of flow. The fluid could be considered random in which case one is considering a diffusion process. Alternately, if the medium is considered as the underlying random mechanism a percolation process is being considered. Subsurface flow is primarily a percolation process and percolation theory is directly applicable. An excellent introduction and summary of percolation theory can be found in Hammersley and Welsh (1980).

On the basis of numerical results, Kirkpatrick (1973) proposed a power law to describe the normalized electrical conductance of a resistor network near the percolation threshold. The flow of fluid through a sandstone/shale network is analogous to the flow of electricity through a resistor network in which some resistors have been removed (sandstone replaced by shales). The relationship between the normalized electrical conductance and the proportion of non-conductive sites (Kirkpatrick, 1973) may be rewritten in our context:

$$\frac{K_e}{K_{ss}} = c(V_{shc} - V_{sh})^t \qquad (2)$$

where V_{shc} is the critical shale fraction, t is an exponent (near 1.5-2.0), and c is a proportionality constant (near 1.5-2.0). The critical shale fraction is the maximum amount of shale beyond which the flow rate will drop dramatically: $V_{shc} = 0.69$, on Figure 2. From Figures 3 and 4 we see that the critical threshold changes with anisotropic shales. As the spatial continuity in the direction of flow increases so does the critical threshold.

The critical threshold can be predicted by percolation theory for some very simple configurations. For example, the critical threshold for random, isotropic shales in a 2-dimensional space is $V_{shc} = 0.5$ (Sykes and Essam, 1964). For spatially correlated heterogeneities in a 3 dimensional space, percolation theory results are not yet established, although simulation results similar to the results presented here exist. The percolation model (2) will be extended to cases where no theoretical threshold value exists and the corresponding parameters (V_{shc}, c, t) will be fitted to the experimental results.

Some Numerical Results:

Two different approaches have been considered to model the relationship between effective permeability and the volume fraction of shale:

1. The power averaging approach which is characterized by a single parameter: the averaging power ω.
2. A percolation model which calls for three parameters: the percolation threshold V_{shc}, an exponent t, and a proportionality constant c.

We are interested in determining the parameters that make each model fit the experimental data best. This can be done by the standard least squares regression procedure. Figure 5 shows the fit of both models to the spatially uncorrelated data presented on Figure 1. Both models achieve a very close fit.

Figures 6 and 7 show the best fitting models for the anisotropic results presented on Figures 3 and 4. In both cases the power average and the percolation model provide very good approximations to the numerical results.

Additional cases, with different anisotropy ratios, were considered to establish the relation between the model parameters (ω, V_{shc}, c, t) and the anisotropy ratio. The anisotropy ratio λ is defined as:

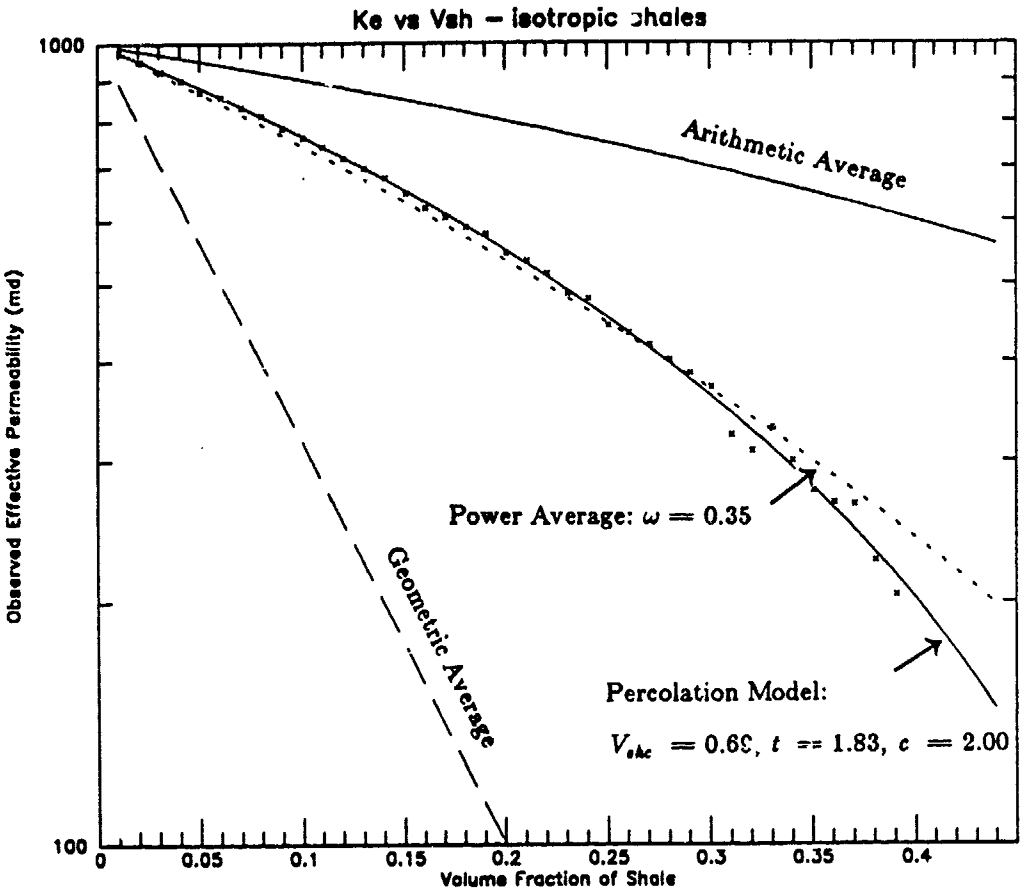

$$\text{Power Average:}\quad K_e = \left(V_{sh} \cdot K_{sh}^{\omega} + (1 - V_{sh}) \cdot K_{ss}^{\omega} \right)^{\frac{1}{\omega}}$$

$$\text{Percolation Model:}\quad K_e = K_{ss} \cdot c \cdot (V_{shc} - V_{sh})^{t}$$

Figure 5: Effective absolute permeability K_e versus shale volume fraction V_{sh}. This graph shows the same results as Figure 2 with more detail for $V_{sh} < 40\%$. A power average model and the percolation theory model are shown to provide an extremely good fit to the experimental results.

12

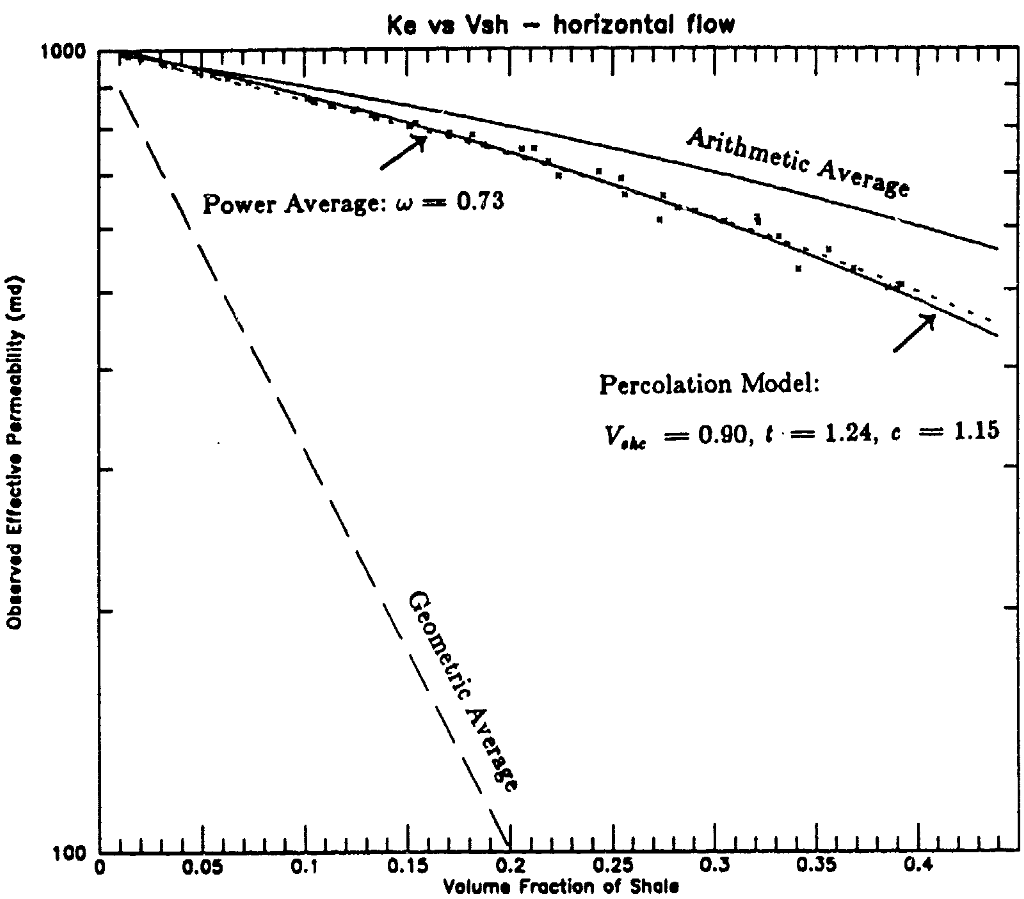

$$\text{Power Average: } K_e = \left(V_{sh} \cdot K_{sh}^{\omega} + (1 - V_{sh}) \cdot K_{ss}^{\omega} \right)^{\frac{1}{\omega}}$$

$$\text{Percolation Model: } K_e = K_{ss} \cdot c \cdot (V_{shc} - V_{sh})^t$$

Figure 6: Horizontal effective absolute permeability K_e versus shale volume fraction V_{sh}. This graph shows the same results as Figure 3 with more detail for $V_{sh} < 40\%$. The power average model and the percolation theory model are again shown to fit well the experimental results.

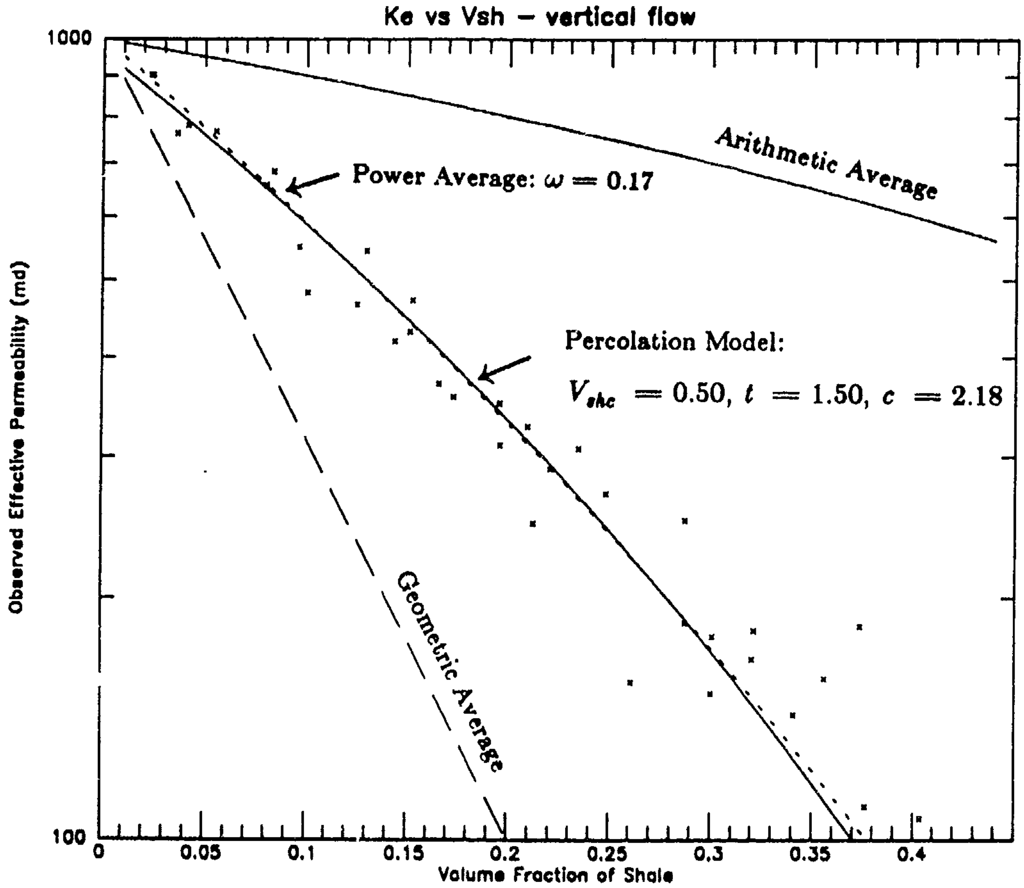

$$\text{Power Average:}\quad K_e = \left(V_{sh} \cdot K_{sh}^{\omega} + (1 - V_{sh}) \cdot K_{ss}^{\omega} \right)^{\frac{1}{\omega}}$$

$$\text{Percolation Model:}\quad K_e = K_{ss} \cdot c \cdot (V_{shc} - V_{sh})^{t}$$

Figure 7: Vertical effective absolute permeability K_e versus shale volume fraction V_{sh}. This graph shows the same results as Figure 4 with more detail for $V_{sh} < 40\%$. The power average model and the percolation theory model provide a good fit to the experimental results.

$$\lambda = \frac{\text{longest shale dimension}}{\text{shortest shale dimension}} \qquad (3)$$

In all our experiments the longest shale dimension corresponds to horizontal directions and the shortest shale dimension to the vertical direction. The effect of horizontal anisotropy is addressed in Appendix B. Figure 8 shows how the averaging power (ω) depends on the anisotropy ratio (λ). The averaging power for horizontal flow (flow in the direction of shale continuity) and vertical flow (flow perpendicular to the plane of shale continuity) are shown on opposite sides of the graph. As the anisotropy ratio increases beyond some maximum, the averaging power is seen to change very little. If λ went to ∞, the arithmetic ($\omega = 1$) and harmonic ($\omega = -1$) averages would be found for respectively horizontal and vertical permeability. However these limit cases would correspond to deterministic shales which are not of interest to this study. The averaging power for vertical flow is seen to be very far from the theoretical minimum of -1. The harmonic average would be obtained when the shales are aligned perfectly opposing flow. This never happens with discontinuous shales since there are always tortuous paths that the fluid can follow through the sandstone. It appears that the geometric average ($\omega = 0$) traditionally used for vertical flow underestimates the effective vertical permeability. Figure 8 corresponds to a finite network size of 20x20x10. In appendix B the effect of the relative shale versus network size is addressed. To consider large anisotropy ratios (λ>7) it would be necessary to use grid sizes larger than 20x20x10. This was not possible with the computer available to this project.

When fitting the percolation model, the percolation threshold is established prior to fitting the other two parameters by least squares regression. The percolation threshold is a clearly defined physical constant and a regression procedure that would fit all three parameters simultaneously would not honor this fact. Figure 9 shows the relationship between the percolation model parameters (V_{shc}, c, t) and the anisotropy ratio (λ). On Figure 9 it appears that for anisotropy ratios λ less than 6, both the critical threshold V_{shc} and the proportionality factor c vary linearly. The power t is found to be constant around 1.71 for vertical flow, and to decrease sharply from 1.71 to 1.25 where it stabilizes for horizontal flow. The physical interpretation of the two parameters c and t and thus their behavior on Figure 9 is not yet understood.

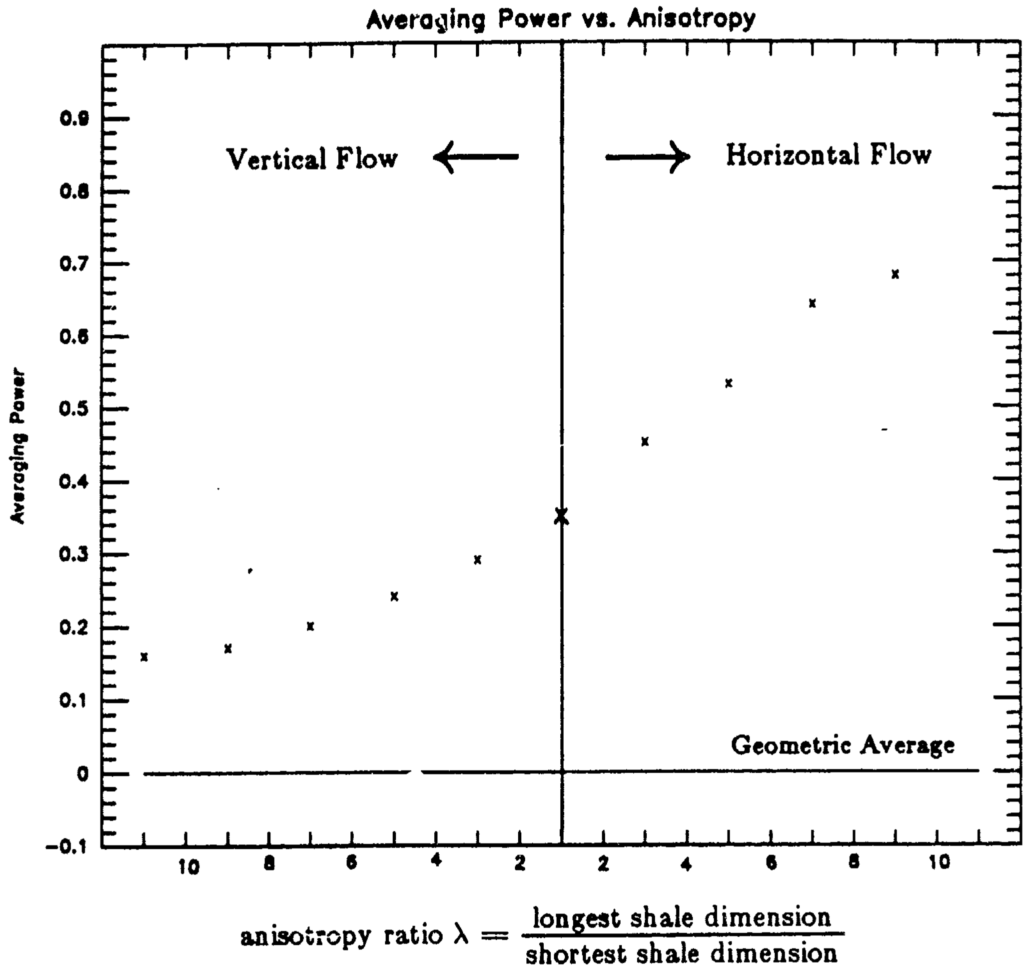

Figure 8: The relationship between the averaging power ω and the anisotropy λ is shown on this Figure. The blocks used in the simulation are 20x20x10. The right side of the Figure is for horizontal flow and the left side is for vertical flow. If the anisotropy of the shales can be inferred then the correct averaging powers can be read from this Figure. Equation 1 can then be used to provide an estimate for the block effective absolute permeability.

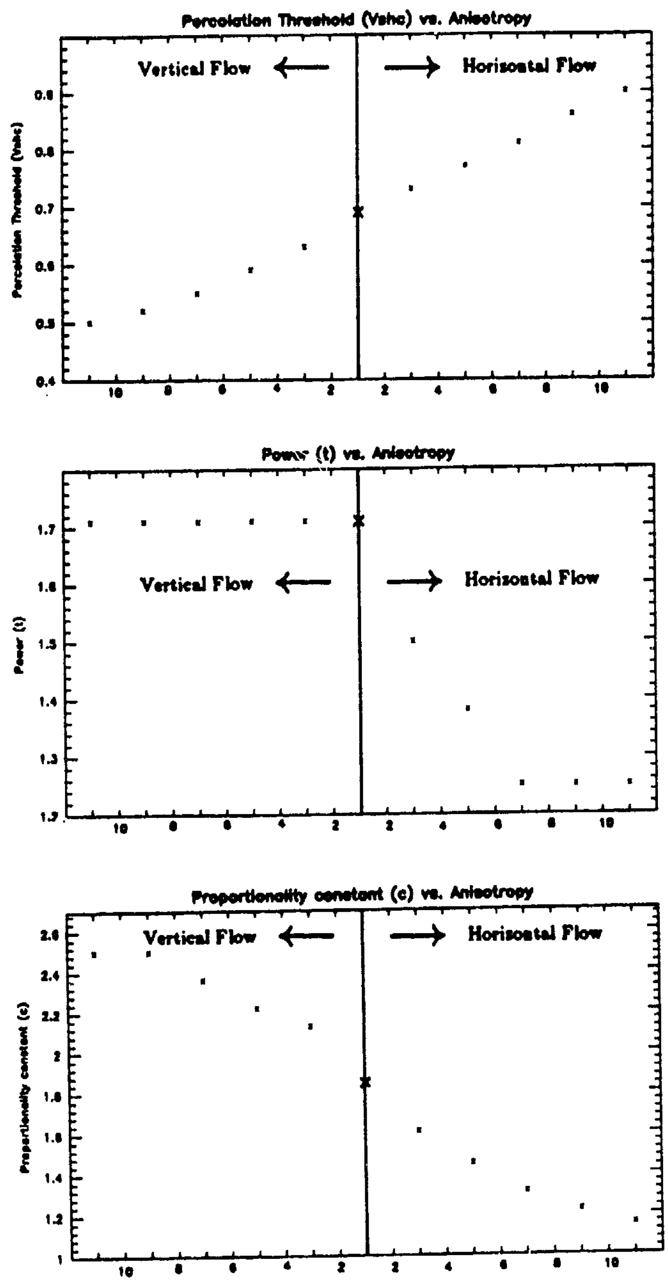

$$\text{anisotropy} = \frac{\text{longest shale dimension}}{\text{shortest shale dimension}}$$

Figure 9: The relationship between the percolation model parameters (V_{shc}, t, c) and the anisotropy λ is shown on this Figure. The simulation conditions are the same as for Figure 8. The right side of the Figure corresponds to horizontal flow and the left side to vertical flow. Knowing λ the appropriate parameters for model 2 can be read from this Figure.

Two different sensitivity analysis are presented in the appendices To summarize the results:

1. *The effect of block size:* For a fixed shale size the effect of changing the block (network, dimensions has been studied. If the shale size is not small with respect to the size of the block then the effective permeability must be adjusted. This correction is required if the shale length is greater than one third of the block length. Details of this correction are given in appendix A.

2. *The effect of horizontal anisotropy:* For a constant λ as defined in equation 3 the effect of anisotropic horizontal dimensions has been studied. Another correction can be applied if the horizontal anisotropy of the shales is known. This correction is discussed in appendix B.

Assuming a large block size and horizontal isotropy are reasonable first approximations. However, when detailed information about the relative block size or horizontal anisotropy is available, it can be used to refine the estimate of the averaging process. Both the power average model and the percolation type model fit well the experimental results. However, one additional question remains:

Which of these two models should be used? There are applications for both models, and reasons to choose one model over the other:

Reasons to use the power average approach:

- The power average is the most parsimonious (1 parameter versus 3). A procedure that requires evaluation of a single parameter (ω) is extremely easy to implement.

- The shale permeability does not have to be set to zero as is required by the percolation model.

- The power averaging algorithm can be extended to a multimodal or continuous distribution of permeability. The percolation model is not easily generalized to the case of a multimodal permeability distribution.

Reasons to use the percolation model:

- The model is continuous until the percolation threshold. This allows estimation of permeability for very shaley sequences.

- Because it relies on 3 parameters rather than one, the percolation model gives the lowest mean squared error when fitting the experimental data.

The drawback of the percolation model is that three parameters must be estimated. Estimating the parameters is complicated because the estimate of one parameter will affect the choice of the others.

The power averaging model appears to be the simplest and most practical. Averaging powers can be estimated from charts such as Figure 8. Then the effective permeability can be obtained from equation 1. The improvements over the traditional arithmetic and geometric averages can be appreciated from Figures 6 and 7.

Conclusions

For sandstone/shale sequences, a major problem is that of averaging the component sandstone and shale permeabilities to obtain block effective permeability. Typically a geometric average $\omega = 0$ is used for vertical permeability and an arithmetic average $\omega = 1$ is used for the horizontal permeability. Results from flow simulation make it clear that this approach can be improved if the anisotropy of the shales is accounted for. Two models have been proposed to account for the shale anisotropy.

The averaging process for absolute permeability in sandstone/shale sequences can be modeled by either a power average or a percolation model. The power averaging model is recommended because of its simplicity and effectiveness. The important aspect of this averaging problem is the presence of two rock components. The preliminary results of this research require certain limiting assumptions: the sandstone and shales are assumed to be respectively homogeneous, and the shales are assumed to be located independently from each other with the same elliptical shape and orientation; however, these ellipsoids are allowed to overlap thus generating spatial correlation. By making the averaging process depend on the spatial anisotropy more information can be used and a better estimate of effective permeability in sandstone/shale sequences can be obtained. Thus, the reservoir model will be more accurate and predictions from flow simulation programs are more likely to reflect future reservoir performance.

Nomenclature

V_{sh} = volume fraction of shale

K_e = block effective permeability (md)

K_{ss} = sandstone permeability (md)

K_{sh} = shale permeability (md)

ω = averaging power ε [−1 , +1]

V_{shc} = critical shale volume fraction

t = a percolation model parameter

c = proportionality constant (unitless)

B = dimensionless block length

ω_{ac} = averaging power corrected for block size

b = block size correction factor

Acknowledgements

The collaboration and support of Prof. A.G. Journel made this research possible. The Stanford Center for Reservoir Forecasting (SCRF) provided the necessary funding.

References

- Desbarats, A.J., "Numerical Estimation of Effective Permeability in Sand - Shale Formations," Water Res. Res., 23,2, 273-286, Feb. 1987
- Deutsch, C.V., "Estimating Block Effective Permeability with Geostatistics and Power Averaging," Submitted to SPE J #015991, 1986
- Eclipse Flow Simulator Manual, ECL, 1984
- Fogg, G.E., "Groundwater flow and sand body interconnectedness in a thick multiple aquifer system," Water Res. Res., 22, 5, 679-694, Oct. 1986
- Haldorsen, H.H., Lake, L.W., "A New Approach to Shale Management in Field-Scale Models," SPE Journal, 447-457, Aug. 1984
- Hammersley J.M. and Welsh D.J.A., "Percolation Theory and its Ramifications," Contemp. Phys., 21, 6, 593-605, 1980
- Journel, A.G., Deutsch, C.V., Desbarats, A.J., "Power Averaging for Block Effective Permeability," SPE Paper 15128, presented at the 56th California Regional Meeting of the SPE held in Oakland, CA, April [illegible] 1986
- Korvin, G., "Axiomatic Characterization of the General Mixture Rule," Geoexploration, 19, 267-276, 1981
- Smith, L., Freeze, R.A., "Stochastic Analysis of Steady State Groundwater Flow in a Bounded Domain 1: One Dimensional Simulations," Water Res. Res., 15,6, 1543-1559, 1979
- Sykes, M.F, Essam, J.W., J. Math Phys., 20, 325- 1964
- Wadman, D.H, Lamprecht, D.E., Mrosovsky, I., "Joint Geological Engineering Analysis of the Sadlerochit Reservoir, Prudhoe Bay Field," J. Pet. Tech., 933-940, July 1979
- Warren, J.E., Price, H.S., "Flow in Heterogeneous Porous Media," SPE Journal, 153-169, Sept. 1961
- Weber, K.J., "Influence of Common Sedimentary Structures on Fluid Flow in Reservoir Models," J. Pet. Tech., 665-672, March 1982

Appendix A: The Effect of Block Size

All numerical flow simulations must consider a finite grid size. In some cases the shales will not be all *small* with respect to the size of the grid block. We know that the effective properties of a bounded medium depend on the ratio of the autocovariance range to the block dimension. This is discussed by Smith and Freeze (1979) for one and two dimensional flow. For three dimensional flow this effect is illustrated by Desbarats (1987).

The size of the shales and the autocovariance range are equivalent when the shale centers are located independently. This is the case for the simulations generated in this paper. Therefore, a dimensionless block length can be defined as the ratio of the block length to the length of the elemental shales:

$$B = \frac{\text{block length}}{\text{shale length}} \tag{A.1}$$

From the numerical results noted above (Smith and Freeze, 1979; Desbarats, 1987) it is known that if B is greater than 2 or 3 there will be no noticeable change in the effective properties. This would suggest that the block size should be selected greater than 3 times the shale size in order to filter out the influence of the grid size. This corresponds to the notion of an REV or representative elemental volume.

In this appendix we are not concerned with grid blocks that are larger than an REV (i.e., $B > 3$). Neither are we concerned with grid blocks smaller than the size of the shales (i.e., $B < 1$) which would correspond to deterministic shales. The main concern is for shales which are neither small nor large with respect to the grid size (i.e., $1.0 < B > 3.0$). This situation will occur in practice when some of the shales are not small with respect to the size of the grid blocks. Therefore, the effect of the block size must be known and handled.

Figure A.1 shows how the averaging power ω varies with the block size B for shales with a fixed 3:1 anisotropy ratio (i.e., $\lambda = 3$). Some interesting remarks:

- For horizontal flow the power ω decreases to an asymptotic minimum as B becomes large. The minimum is reached around B=3.
- Practical dimensionless block lengths for the vertical direction are always large (i.e.,

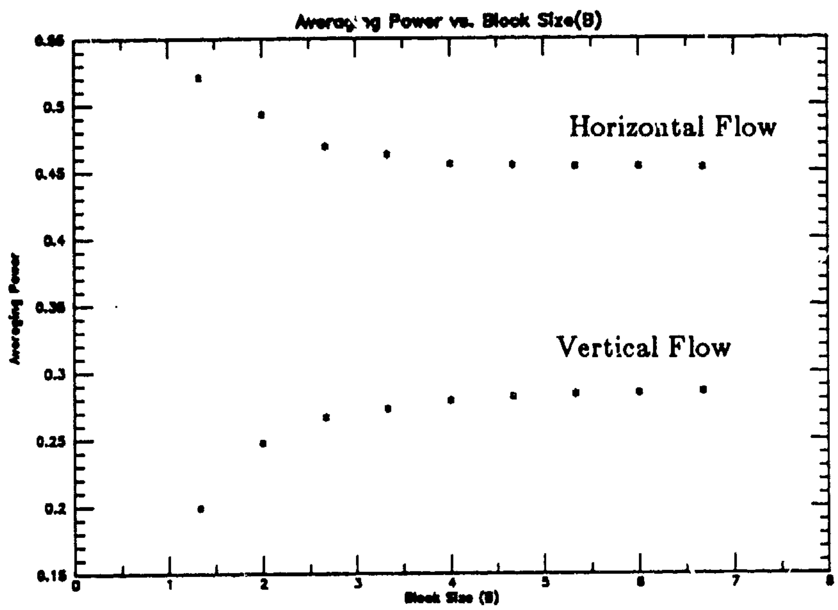

Figure A.1: The averaging power ω versus the relative horizontal block size (B). The results for both horizontal and vertical flow are shown. For blocks with horizontal dimensions larger than three times the shale length ($B=3$) the averaging power stabilizes.

B>10). On Figure A.1 we are seeing the effect of the horizontal dimensionless block length on the vertical flow behavior. The averaging power ω increases to a maximum as B becomes large (B>3).

From this Figure we can make some general conclusions about the effect of the block size. First, we see that if the block length is less than 3 times the shale length the effective permeability is affected. For horizontal flow the effective permeability is greater than that obtained for the "large block" domain (B>3), conversely the vertical permeability is smaller than that for the "large block" domain.

The effect has been shown for only one anisotropy ratio λ=3. However, it is clear that this effect will occur for all anisotropy ratios. To account for this effect a correction to the averaging power of the following form is proposed:

$$\omega_{ac} = b \cdot \omega \tag{A.2}$$

where ω_{ac} is the corrected averaging power, ω is the limit averaging power corresponding to the large block, and b is a block correction factor. The block correction factor (b) can either be obtained directly from charts or Figures such as A.1, or a mathematical relation of the following form could be used:

$$b = 1 + a \cdot e^{-B} \tag{A.3}$$

where a is a constant that measures the amount of correction needed. As the relative block size B becomes large (B > 3) the block correction factor b will be equal to 1. The constant a will be positive for horizontal flow and negative for vertical flow. For example the constant a would be +0.60 and -1.11 for the horizontal flow and vertical flow results shown on Figure A.1. The resulting models are shown on Figure A.2.

The effect of the block dimension relative to the shale dimension has been addressed. If the size of the block is small or if the shales are large, the limit averaging power corresponding to large blocks must be corrected. A negative exponential correction is proposed to provide this correction.

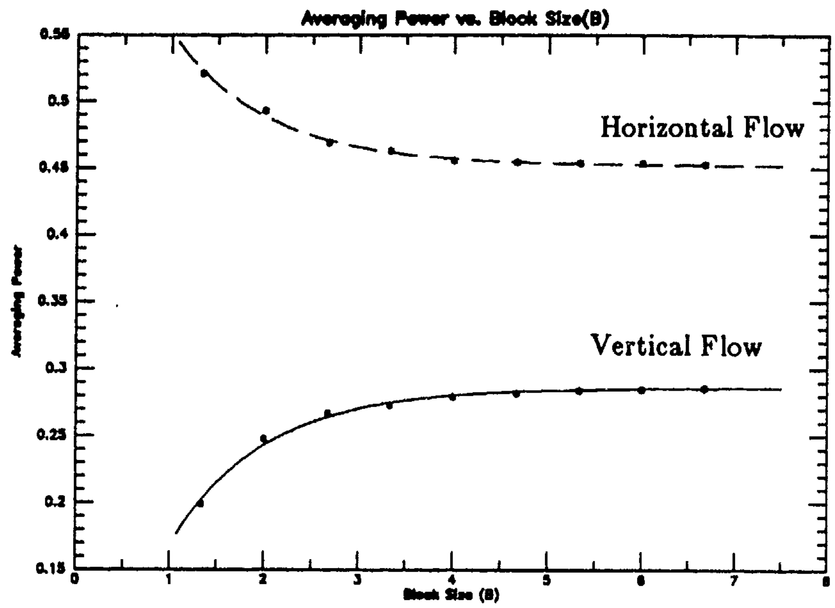

$$\omega_{ac} = (1 + a \cdot e^{-B}) \cdot \omega$$

Horizontal Flow: $\omega = 0.45$ and $a = 0.60$

Vertical Flow: $\omega = 0.29$ and $a = -1.11$

Figure A.2: The averaging power ω versus the relative block size (B). The results of Figure A.1 are modeled with an exponential correction function.

Appendix B: The Effect of Horizontal Anisotropy

This appendix illustrates the effect of anisotropic horizontal shale length on the directional permeability. The anisotropy ratio λ as defined in equation 3 (longest over shortest shale dimensions) will be kept constant at $\lambda = 10$ and the second horizontal length will be progressively reduced.

When the shales are anisotropic in the horizontal plane the effective permeability will be different for each of the three grid directions. Figure B.1 shows the averaging power ω versus the horizontal anisotropy for each grid direction (recall that λ is fixed at 10). Some remarks:

- The permeability in the direction of maximum shale continuity or length is the largest and the permeability in the direction of minimum shale continuity is the smallest.
- The vertical permeability increases (for a given λ) with increasing horizontal anisotropy.

In practice there may be information on the directional horizontal dimension of the shales. In this case, the directional permeability can be corrected in the manner described above.

26

SPE 17264

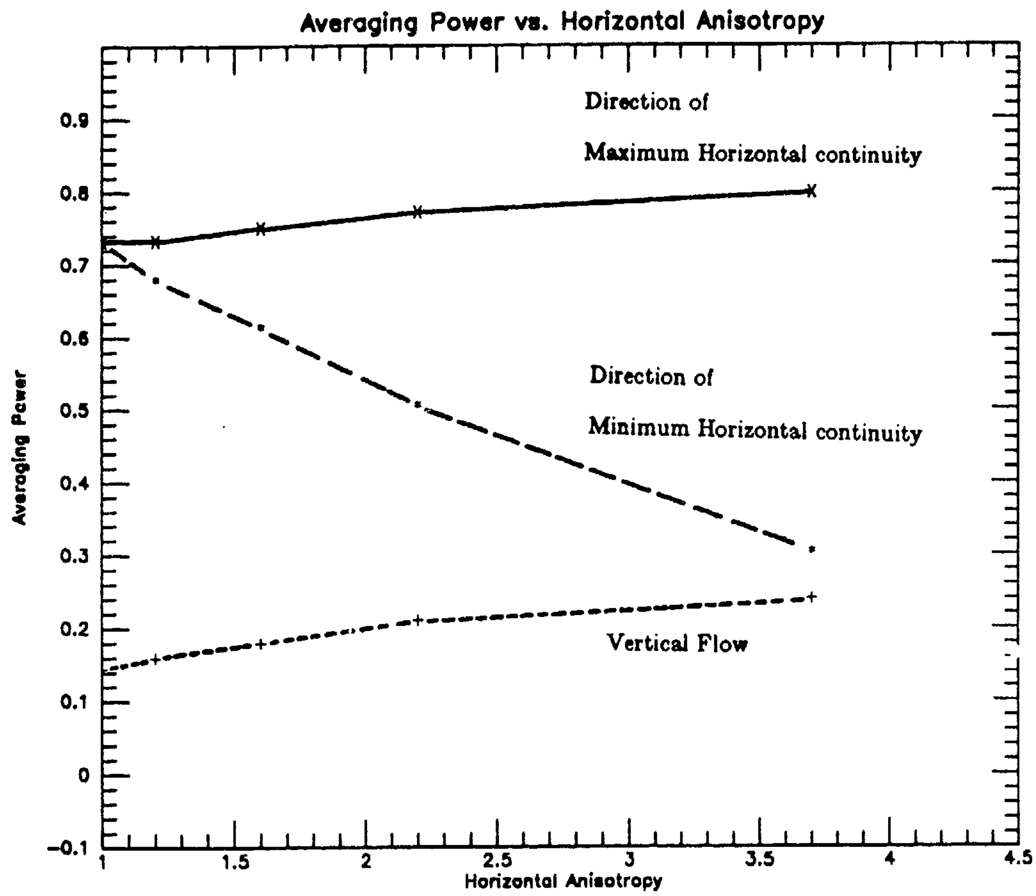

$$\text{horizontal anisotropy} = \frac{\text{longest horizontal dimension}}{\text{shortest horizontal dimension}}$$

Figure B.1: The relatio'ship between the averaging power ω and the horizontal anisotropy is shown. 'he vertical to horizontal anisotropy ratio as defined in equation 3 is held constant at 10. The effect of horizontal anisotropy on the averaging for all three block directions is shown.